LAWRENCE
LIVERMORE
NATIONAL
LABORATORY

LLNL-PROC-574692

A Hybrid Analytical Model for Radiography Cone Beam Effects

H. Wang, V. Tang

August 17, 2012

ASNT Fall Conference 2012
Orlando, FL, United States
October 29, 2012 through November 2, 2012

Disclaimer

This document was prepared as an account of work sponsored by an agency of the United States government. Neither the United States government nor Lawrence Livermore National Security, LLC, nor any of their employees makes any warranty, expressed or implied, or assumes any legal liability or responsibility for the accuracy, completeness, or usefulness of any information, apparatus, product, or process disclosed, or represents that its use would not infringe privately owned rights. Reference herein to any specific commercial product, process, or service by trade name, trademark, manufacturer, or otherwise does not necessarily constitute or imply its endorsement, recommendation, or favoring by the United States government or Lawrence Livermore National Security, LLC. The views and opinions of authors expressed herein do not necessarily state or reflect those of the United States government or Lawrence Livermore National Security, LLC, and shall not be used for advertising or product endorsement purposes.

A Hybrid Analytical Model for Radiography Cone Beam Effects

Han Wang[1], and Vincent Tang[1]
[1]Lawrence Livermore National Laboratory
7000 East Ave Livermore, CA 94550
(925) 422-8717; e-mail wang61@llnl.gov

ABSTRACT
An improvement to the inversion algorithm based on the maximum entropy method (MEM) proposed by Wang et al [1] is presented. The original algorithm aimed to remove unwanted effects in fast neutron imaging which result from an uncollimated source interacting with a finitely thick scintillator. The algorithm takes as an input the image from the thick scintillator (TS) and outputs a restored image which appears as if taken with an infinitesimally thin scintillator (ITS). However, the inversion process is heavily dependent on a linear model relating the ITS image to the TS image and in the inversion sequence, any error or noise in this model is carried through to the reconstructed image. Improving on the work of [1], we present a new hybrid semi-analytical approach to generate a more accurate and less noisy linear model. The new hybrid model increases accuracy by incorporating intra-scintillator scatter while lowering computation requirements by splitting the generation of the linear model into two phases.

INTRODUCTION
The unique ability of fast neutron imaging to resolve low-Z objects shielded by high-Z materials allows for additional radiographic possibilities of shielded objects, [2]. However, fast neutron imaging has traditionally relied on the use of a collimated beam which required high intensity non-portable sources. In our previous paper, [1], we demonstrated the feasibility of uncollimated neutron imaging by correcting for the cone beam effect (CBE) of uncollimated source beams via post processing. The original algorithm required three parts. First, a background image which was then processed by a residual boosted support vector regression smoothing algorithm, [3-5], to produce a Bayesian prior; second, a linear model which expresses the inter-neighbor pixel dependencies due to the CBE, and third, an inversion algorithm based on the maximum entropy method (MEM) to remove the effects of the linear model from the actual image, [6].

We found that out of the three components, the linear model factored most into reconstructed image quality. This makes intuitive sense as it is the 'link' between the uncollimated acquired image and the 'collimated' acquired image. Capturing on this insight, we derived a new linear model which accounts for the scattering within the scintillator scattering as well as the linear attenuation experienced by neutrons passing through the scintillator.

CONE BEAM EFFECT
The problem experienced by uncollimated neutron imaging is the cone beam effect, which itself is a generalization of the concept of geometric unsharpness. The effect is dependent on the thickness of the radiation detector used, and the angle formed by the source to detector ray. When the source to detector distance is within an order of magnitude compared to the detector thickness, CBE becomes the prominent factor in image degradation.

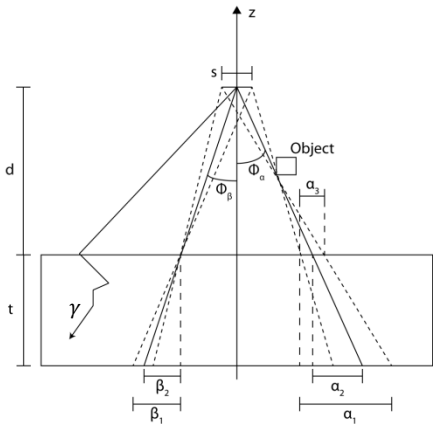

Figure 1

As shown in Figure 1, fixing source to detector distance, d, and detector thickness, t, the CBE is characterized by Φ, the angle between the ray passing through the entry point and the z axis. A neutron entering at the surface can terminate anywhere in the ray which intersects the scintillator. Since the pixelated detector array is parallel to the entry surface of the scintillator, each incident particle is subject to a blurring effect which can only be defined probabilistically. Since the angular dependence on Φ is rotationally invariant about the z axis, any line from the source to a point on the surface of the detector can be rotated about the z axis to create a cone which is subject to the same blurring effect. It is this conical symmetry which lends this particular geometric unsharpness its name, the cone beam effect.

However, the above model only accounts for the first order effect of linear attenuation. A more complete picture would follow from ray α which is subject to intra-scintillator scattering as well. This expands the set of possible termination points of the neutron, by defining a scalar field of termination probabilities which decreases with both penetration depth and distance away from the linear attenuation ray.

The best way to mitigate the attenuation and scatter blurring of the CBE is to reduce the thickness of the detector and from Figure 1, we see that this approach will yield an infinitely sharp point, when the detector becomes infinitesimally thin. For a feature not focused at the surface of the detector, taking $d \to 0$ will not recover a completely sharp image, α_3, but the resulting image quality is still superior to the original. Thus, we focus our efforts on relating the image that is taken with an ideal infinitesimally thin scintillator (ITS) to an image taken by a scintillator of thickness, t, Eqn. 1.

$$Ax = y \qquad \text{Eqn. 1}$$

Here, A is the linear model, x is the ITS image and y is the thick scintillator image. x and y are both vectors created by vectoring the pixels into column-major order. After defining A, we invert the model between the two images on the thick scintillator image to remove the CBE. It should be noted that the Eqn. 1 is extremely ill conditioned and a regularization technique such as MEM is necessary during the actual inversion process.

SIMPLE LINEAR ATTENUATION MODEL

The simple linear attenuation model was based on a full discrete treatment. First we partitioned the scintillator into voxels, volumetric pixels. Next, we assumed that the distance to first interaction of a neutron in the scintillator is an exponential random variable with its mean equal to the mean free path of the neutron. Finally, we assumed that all neutrons give up all their energy on the first interaction so there is no scattering within the scintillator.

Working off the above assumptions, we defined a bijection between each pixel in the observed image and a voxel on the scintillator, Figure 2.

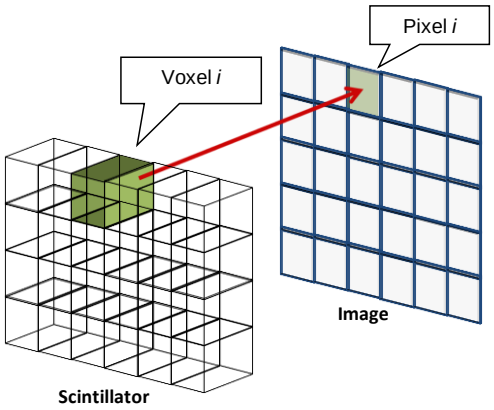

Figure 2

If any neutron interacts with the scintillator in voxel i, we assume pixel i increases its intensity count by a constant factor. The prior assumption is justified because each voxel interacts with enough neutrons to ensure central limit convergence, and the ratio of standard deviation of neutron count to mean neutron count is less than 0.05.

In the framework of the discrete voxel scintillator, we wish to solve the number of neutrons incident on each voxel given the number of neutrons terminating in each voxel. Neglecting the intensity variance, the number of incident neutrons is exactly the response of the ideal infinitesimally thin detector. Thus removing the cone-beam effect is equivalent to solving for the number of incident neutrons.

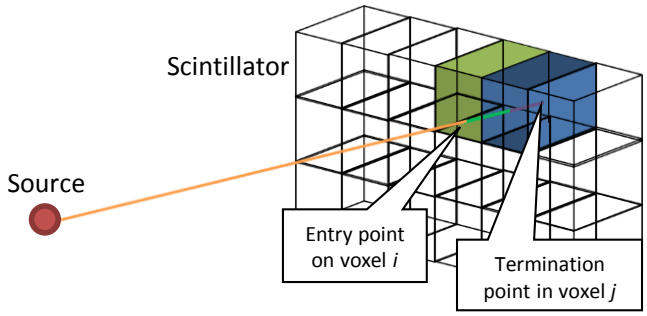

Figure 3

Given our voxel scintillator model, we now clarify our linear model, Eqn. 2. We redefine x as the vector consisting of the incident counts for each voxel, and y as the vector consisting of the termination counts for each voxel. Now A becomes the probability transfer matrix (PTM) between incident voxel and termination voxel, such that $[A]_{ij}$ denotes the probability a neutron incident on voxel i will terminate in voxel j, Figure 3.

Instead of using an analytical approach, we generate A via Monte Carlo simulation through the following algorithm.

FOR each voxel i
    FOR n = 1 to N
        Sample α_n, the entry point on voxel i's surface
        Sample β_n , the emission point on the source's surface
        Sample e_n, the neutron energy for neutron }n
        Calculate λ_n given e_n
        Sample p_n,the penetration distance, given λ_n
        Ray Trace from α_n text to β_n text and find ψ_n,text the termination point, given p_n
        Calculate which voxel $j \ni \psi_n$
        Add $\frac{1}{N}$ to $[A]_{ij}$
    ENDFOR
ENDFOR

The result of this algorithm is a PTM that has been calculated by following the linear attenuation of N particles per pixel. For smooth convergence, N is recommended to exceed 1e8.

HYBRID ANALYTICAL ATTENUATION AND SCATTER MODEL

The more complicated hybrid analytical model seeks to construct not the probability transfer matrix between incident voxel and termination voxel but the energy transfer matrix. This matrix describes the expected energy deposited in voxel i given a neutron incident in voxel j. For computational feasibility, we generated this model through separation of the intra-scintillator response and the entry geometry.

For the intra-scintillator response, we utilized MCNP in conjunction with pulse tallies to estimate the energy deposited within the scintillator given a fixed entry point and angle, [7]. This discrete grid is an estimate of the field of expected energy deposited given incident neutron which we term T. Through this model, we assume a monotonic relationship between energy deposition and optical photon generation.

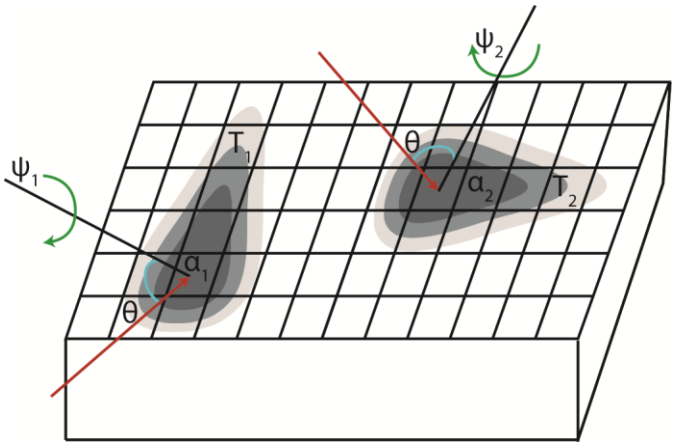

Figure 4

$$T(u, v, w, \alpha, \theta, \psi) = E(\text{Energy deposited at } (u, v, w) | \alpha, \theta, \psi)$$

Looking at Figure 4, we see that for two particles with $\theta_1 = \theta_2,\ \psi_1 = \psi_2,$ and $\alpha_1 \neq \alpha_2, T_1 = T_2$ under translation by $(\alpha_1 - \alpha_2)$. In addition, for two particles with $\theta_1 = \theta_2,\ \psi_1 \neq \psi_2,$ and $\alpha_1 = \alpha_2, T_1 = T_2$ under rotation by $(\psi_1 - \psi_2)$. Thus, we do not need to simulate every possible set of α, θ and ψ. We can set α, and ψ to base values while varying θ to get T for all possible entry angles and then performs translations and rotations of our original calculations to return T for any α, θ and ψ of interest. We use this geometrical symmetry to tie the intra-scintillator response to the entry geometry.

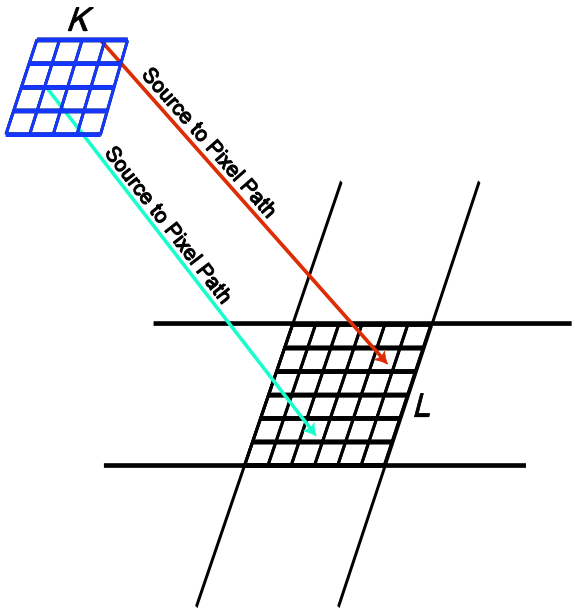

Figure 5

For our base values, we set $\alpha_0 = (0,0,0)$ and $\psi_0 = 0$, and define, $T_0(u, v, w, \theta) = T(u, v, w, \theta, \alpha_0, \psi_0)$. We run this simulation for $\theta \in \left[0, \frac{\pi}{2}\right)$, utilizing MCNP and an F8 pulse grid of four times the density as our original voxel mesh.

Since the discrete grid does not possess the resolution we require, we parametrically fit a third order polynomial on T_0 in u,v, and θ (the MCNP pulse tallies already integrate over w) which we define as T_f.

$$T_f(u,v,\theta) = a_1u + a_2u^2 + a_3u^3 + b_1v + b_2v^2 + b_3v^3 + c_1\theta + c_2\theta^2 + c_3\theta^3$$

Next we impose a $K \times K$ square mesh over the source's surface and a $L \times L$ square mesh over pixel i, Figure 5. We calculate θ_j for each source/entry combination, j. Next, we translate and rotate $T_{f,j}(u,v,w,\theta_j)$ to match the entry point and ψ_j for each source/entry combination. Finally we evaluate $T_{f,j}$ at every corner of each neighboring voxel p and take the mean of the corners. We add this mean to voxel p's total for each j. After we have completed that, we normalize to one by multiplying each pixel p's value by $\frac{1}{4K^2L^2}$.

Algorithmically the model can be described as follows.

FOR each $\theta \in \left(0, \frac{\pi}{2}\right]$
    Calculate T_0
ENDFOR

Fit T_f given all the T_0's.

FOR each voxel i
    FOR $k = 1$ to K^2
        FOR $l = 1$ to L^2
            Calculate θ
            FOR each voxel p in neighborhood
                Evaluate T_f at each of voxel p's corners
                Take the mean, m, of all 4 corners
                Add $\frac{m}{4K^2L^2}$ to $[A]_{ip}$
            ENDFOR
        ENDFOR
    ENDFOR
ENDFOR

ALGORITHM COMPLEXITY

For given a $K \times K$ source mesh and a $L \times L$ pixel mesh, we have K^2L^2 source/pixel pairs. For each source/pixel pair, we have to perform 1 translation and 1 rotation. Next, we need to evaluate the corners of all relevant neighbors. Assuming the farthest relevant neighbor is P pixels away, this becomes a $4P^2$ operation. Assuming a total number of pixels I, the algorithmic complexity required to calculated a new PTM is $O(K^2L^2P^2I)$, which satisfactorily remains in polynomial time. The algorithmic complexity for calculating T_f given differing incident angles is $O(ZN)$, where Z denotes the number of mesh points in θ and N denotes the total number of neutrons simulated per θ.

CONCLUSION

In conclusion, we have proposed a new model for divergent neutron beam behavior inside a scintillator. Improving on previous work, the new model accounts for intra-scintillator scattering as well as linear attenuation. Currently, we are working on generating the MCNP input decks as well as experimenting with the loss functions which control our parametric fits. Future work will entail a full evaluation of the hybrid analytical model against the simple attenuation model, and a comparison of reconstruction results based on an objective metric such as RMSE.

AWKNOWLEDGMENTS

We thank Jim Hall, Brian Rusnak, Jim McCarrick, and Phil Kerr at LLNL for discussions and guidance on neutron imaging as well as the loan of imaging equipment and facilities. This work was supported in part by the US. Department of Energy Na-22 Office of Nonproliferation Research and Development under the Radiological Source Replacement program and was performed under the auspices of the U.S. Department of Energy by Lawrence Livermore National Laboratory under Contract DE-AC52-07NA27344.

REFERENCES

1. H. Wang, V. Tang, J. McCarrick, and S. Moran, "Reconstruction Algorithm for Point Source Neutron Imaging through Finite Thickness Scintillator", *Nuclear Instruments and Methods A*, DOI:10.1016/j.nima.2012.07.018
2. J. Hall, B. Rusnak, P. Fitsos, High-energy neutron imaging development at LLNL in 8th world conference on neutron radiography, no. 8th, Gaithersburg, MD., 2006.
3. C. Chang, C. Lin, LIBSVM: a library for support vector machines, 2001.
4. C. Cortes, V. Vapnik, Support-vector networks, Machine Learning 20 (1995).
5. A. J. Smola, B. Scholkopf, A tutorial on support vector regression, Statistics and Computing 14 (2004)
6. S. F. Gull, G. J. Daniell, Image-reconstruction from incomplete and noisy data, Nature 272 (1978).
7. MCNP X-5 Monte Carlo Team, MCNP a general purpose Monte Carlo n-particle transport code, Tech. rep., Los Alamos National Laboratory (2003).